



## Article

# Dental X-ray Identification System Based on Association Rules Extracted by k-Symbol Fractional Haar Functions

Mona Hmoud AlSheikh <sup>1</sup>, Nadia M. G. Al-Saidi <sup>2</sup> and Rabha W. Ibrahim <sup>3,\*</sup>

<sup>1</sup> Physiology Department, College of Medicine, Imam Abdulrahman Bin Faisal University, Dammam 34212, Saudi Arabia

<sup>2</sup> Department of Applied Sciences, University of Technology, Baghdad 10066, Iraq

<sup>3</sup> Mathematics Research Center, Department of Mathematics, Near East University, Near East Boulevard, TRNC Mersin 10, Nicosia 99138, Turkey

\* Correspondence: rabhaibrahim@yahoo.com

**Abstract:** Several identification approaches have recently been employed in human identification systems for forensic purposes to decrease human efforts and to boost the accuracy of identification. Dental identification systems provide automated matching by searching photographic dental features to retrieve similar models. In this study, the problem of dental image identification was investigated by developing a novel dental identification scheme (DIS) utilizing a fractional wavelet feature extraction technique and rule mining with an Apriori procedure. The proposed approach extracts the most discriminating image features during the mining process to obtain strong association rules (ARs). The proposed approach is divided into two steps. The first stage is feature extraction using a wavelet transform based on a k-symbol fractional Haar filter (k-symbol FHF), while the second stage is the Apriori algorithm of AR mining, which is applied to find the frequent patterns in dental images. Each dental image's created ARs are saved alongside the image in the rules database for use in the dental identification system's recognition. The DIS method suggested in this study primarily enhances the Apriori-based dental identification system, which aims to address the drawbacks of dental rule mining.

**Keywords:** k-symbol; fractional calculus; Caputo derivative; Haar function; image processing



**Citation:** AlSheikh, M.H.; Al-Saidi, N.M.G.; Ibrahim, R.W. Dental X-ray Identification System Based on Association Rules Extracted by k-Symbol Fractional Haar Functions. *Fractal Fract.* **2022**, *6*, 669. <https://doi.org/10.3390/fractalfract6110669>

Academic Editors: Xuefeng Zhang, Driss Boutat and Dayan Liu

Received: 23 September 2022

Accepted: 8 November 2022

Published: 11 November 2022

**Publisher's Note:** MDPI stays neutral with regard to jurisdictional claims in published maps and institutional affiliations.



**Copyright:** © 2022 by the authors. Licensee MDPI, Basel, Switzerland. This article is an open access article distributed under the terms and conditions of the Creative Commons Attribution (CC BY) license (<https://creativecommons.org/licenses/by/4.0/>).

## 1. Introduction

Advancements in computer networks and mobile technology have a great impact on generating intelligence knowledge from large databases in the era of big data. High dimensionality and unstructured features are common features of databases from several business fields.

Learning enormous databases is a crucial part of the machine learning process. Humans constantly adapt to new situations on a regular basis; learning involves remembering, adapting, and generalizing. Because it requires both information and intellect, the learning process is crucial [1]. The quality of the input data and the type of learning are factors that influence machine learning performance. Data pre-processing is necessary for a machine learning algorithm to handle noisy input and assure output quality and a smooth learning process [2]. Statistics cleansing, data transformation, feature extraction, and feature selection are the most common data tasks included in the document pre-processing phase of learning procedures.

Feature extraction is considered to be the main procedure that moves the output of the prediction process in machine learning, as it extracts the relevant structures to reduce the process time and the space of the problem. Moreover, the quality of the images that are being processed has an impact on the classification algorithm. Any available noise may affect the performance of the achievable accuracy of classification models. For this reason, efficient feature extraction before learning is considered to be an important step in

any classification algorithm to reduce model overfitting and establishing efficient learning due to extracting the efficient attributes in data processing, which are considered during the learning process. The output of the efficient feature extraction methods is combined with a complete set of feature vectors and sent to the grouping algorithm for preparation purposes to obtain classification outputs.

Several image feature extraction methods have been developed by researchers for different approaches of image identification and classification. One of these methods of image feature extraction, which is used to recognize images from a dataset prior to the learning process, is the wavelet transform method. The wavelet transforms using a mathematical model to extract the most relevant features in an image. The main function of wavelet transforms is the recursive decomposition at each level of the input image into a low-pass coarse approximation with high-pass detail information.

The quick development of internet technology results in huge numbers of generated images every day, which need efficient mining systems to automatically analyze and review the knowledge from these images. AR mining has been effectively utilized in many industrial and business fields [3]. AR mining is considered to be one of the data mining techniques that is used to extract associations among different item sets in transactional databases. These associations characterize the rules that assist users in decision making. High-confidence ARs indicate the harmony of relevance for the conceptions of users. AR is a classification algorithm that was proposed by Liu, Hsu, and Ma to find rules that can be applied as a classification model [4–10]. By creating a novel DIS utilizing the wavelet image extraction approach, AR mining, and the Apriori algorithm, the problem of identifying teeth images was examined in this study. The proposed system employs feature extraction and AR mining with an Apriori algorithm. Based on learning rules, the extracted features in the training dataset are used to define their significances. The rule's body is then pruned of all irrelevant correlations, which are repetitive, and rules connected with only one feature value are kept. The AR assures that the learned rules have no common training instances, reducing the number of features in the result set that are identical.

Data mining is growing very fast as a research area in computer science. Knowledge discovery in databases (KDD) has been strongly considered as an attractive research field in the computing area. KDD aims to discover more useful data that are stored in transactional databases. Moreover, AR mining is one of the well-known approaches of knowledge discovery. AR mining can efficiently extract the most exciting relations among different data attributes for decision making.

The dental photographs produced at dental clinics and hospitals include valuable information that may be revealed to consumers looking at these images. Image mining algorithms that can automatically analyze the knowledge from these images are therefore greatly needed. Dental image analysis and diagnosis have become crucial processes, necessitating computer-assisted DIS to assist in this work. Because it is regarded as a valid and trustworthy form of identification, dental identification is a crucial standard procedure in civilized society. The DIS compares any pre-mortem records with the charted records. Organizations now use a variety of identifying techniques [11]. Every technique, meanwhile, has its own benefits and disadvantages.

A wavelet family or basis, including the Haar wavelet, is made up of a series of downscale “square-shaped” functions. Similar to Fourier analysis, wavelet analysis allows the illustration of a target function across an interval in relation with an orthonormal basis [12]. The Haar wavelet has a technical drawback in that it is not continuous and cannot, therefore, be differentiable. However, this characteristic may be advantageous for the analysis of discrete data (signals, videos, and images with abrupt transitions), such as the detection of tool failure machines. Recently, different generalizations using different types of fractional calculus, including the classical and modern differential and integral operators, were given in [13–16].

In this study, we shall make an extra generalization for the fractional Haar functions by using the concept of  $k$ -symbol calculus [17]. Basically, this type of calculus focuses on

extending gamma functions. We illustrate the derivation and numerical example. In the suggested technique, the most discriminating dental image features during the mining process to obtain strong ARs are used and are applied for an effective DIS.

## 2. Related Works

The digesting, analyzing, and producing of information from data can be utilized to find links between significant relational databases. This process is considered to be the main object of data mining or knowledge discovery. Data mining allows handlers to explore data from different measurements and mine the associations between databases. Image data are considered to be the basis of much research work, such as in medicine, where data mining is becoming very important. Image mining is an interdisciplinary research area, including different methodologies such as data mining and computer vision [18]. Currently, a huge number of medical images are generated daily and are analyzed by a radiologist for the diagnosis process [19]. This has motivated researchers to design an enormous number of medical image databases. The achievement of image analysis increases the demand to expand the automatic digital decision making that combines multiple techniques such as image processing and data mining. Data mining is an active research area in data science that aims to discover useful data from a collection of data stored in transactional databases. Another approach of data mining is referred to as image mining. Image mining deals with data mining in which the images are considered to be the data [20].

The image mining approach of data mining is distributed with the extraction of designs from metaphors that are stored in a large gathering of images. Obviously, image mining has different features comparable with image processing or with computer vision techniques because image mining focuses on the extraction of image patterns from large groups of images [21,22], while image processing and computer vision techniques focus on the understanding of image features from images. There are some similarities between image mining and content-based image retrieval [23].

In 1993, Agrawal et al. [24] proposed the algorithm of AR mining for the first time. Regarding image mining, in 2002 Hsu et al. [25] proposed a survey of several image mining frameworks for image mining as well as the current advancements in image mining. Another approach, which used a combination of ARs with the rough set theory to create a joining associative classifier for medical image classifications, was proposed by Jiang Yun et al. in 2005 [26].

In 2005, Tseng et al. [27] used a new method for image classification based on multi-level AR mining. The main stages of this method included three phases. In the first stage, a conceptual object hierarchy was created, in the second stage the classification rules were discovered, and in the third stage the classification of images was obtained. Better performance was achieved compared with other relevant approaches in terms of accuracy. In another approach, in 2008 Reberio et al. [28] proposed a new method for diagnosing dental images using AR mining. The method succeeded in reducing the mining complexity due to combining the selection with discretization into one step. This method suffers from redundant features, which need to improve the feature extraction methods.

In 2009, Ribeiro M et al. [29] proposed a new approach to support the content-based image retrieval (CBIR) based on the AR algorithm. The reason of applying the ARs is to reduce the image feature dimensionality to enhance the precision of the image retrieval. Moreover, a few future research approaches were suggested for image mining in this study. In 2010, Rajendran et al. [30] proposed a novel brain tumor classification method as a hybrid image mining based on using ARs. The proposed method achieved 93% accuracy after using AR mining to classify CT scan brain images into three classes. In the same approach, in 2011 Da Silva et al. [31] proposed improved CBIR based on using a genetic algorithm as a feature selection method. Meanwhile, for enhancing the retrieval accuracy, a wrapper strategy is utilized to discover the best reduced feature sets. The achieved results have better accuracy compared to relevant methods.

Moreover, an image data mining framework was proposed by Sahu M et al. in 2012 [18] based on image texture content such as energy, entropy, and contrast. The results achieved a precision of 0.6. However, the achieved results needed more improvement with the use of other image feature types. AR mining is a well-known method that is used to effectively extract interesting relations among different data attributes, which helps in decision making. Another approach based on using ARs was proposed by Abdi et al. in 2013 [32] for the classification of erythematous-squamous diseases. The model used support vector machines (SVMs) with particle swarm optimization (PSO). The method had two phases: the first phase was the image feature extraction and selection, while in the second phase the AR was used to select the optimal features. The achieved classification rate was 98.91%, showing the robustness of the classification of erythematous-squamous diseases. For classifying medical images, in 2014 Mangat et al. [33] applied the dynamic particle swarm optimization (PSO) algorithm to determine the ARs to classify the input medical images. The advantage of PSO is the ability to deal with a large number of attributes and with a large searching space. Moreover, in 2016 Deshmukh et al. [5] proposed a new image mining approach to extract the highly associated rules from dental image textured features. The proposed method consists of three stages: image feature extraction, optimization for feature selection, and finally the creation of an input image transaction database. This method was used to develop an algorithm to extract strong ARs to enhance the achieved results. Experimental results have shown that the image mining is sufficient to efficiently give strong ARs.

Although several researchers have proposed different methods for image mining to find more efficient ARs, image mining is still a challenging task. In this proposed method, AR mining with the Apriori algorithm is used to extract the frequent patterns in similar images. These rules can be applied to effectively identify dental images. In the suggested process, the general wavelet transforms the feature extraction used during the mining process to extract the strongest rules. The proposed DIS works in two phases: first, the wavelet image extraction and, second, AR mining by means of an Apriori system. The proposed Apriori algorithm is used to generate operative and highly correlated ARs from dental images. The images are pre-processed using both noise removal with cropping and image enhancement operations. The extracted features from cleaned images are applied to the mining phase of the joining associative classifier.

### 3. Mathematical Design by k-Symbol FHF

Haar functions form an orthonormal basis for the space of integral functions  $L_2[0, 1)$ . Therefore, all functions in this space satisfy the power series:

$$\phi(\tau) = \sum_{n=0}^{\infty} \varphi_n \tilde{h}_n(\tau)$$

where  $\tilde{h}$  indicates the Haar functions [34]:

$$\tilde{h}(\tau) = \begin{cases} 1 & 0 \leq \tau < 1, \\ 0 & \text{otherwise.} \end{cases}$$

The Caputo's differential operator of the function  $\phi$  is defined as follows:

$$\begin{aligned} {}^C D_{\tau}^{\alpha} \phi(\tau) &= \frac{1}{\Gamma(1-\alpha)} \int_0^{\tau} \frac{\phi'(\zeta) d\zeta}{(\tau-\zeta)^{\alpha}} \\ &= \frac{1}{\Gamma(1-\alpha)} \int_0^{\tau} \frac{\sum_{n=0}^{\infty} \varphi_n \tilde{h}'_n(\zeta) d\zeta}{(\tau-\zeta)^{\alpha}} \\ &= \frac{1}{\Gamma(1-\alpha)} \sum_{n=0}^{\infty} \left( \int_0^{\tau} \frac{\varphi_n \tilde{h}'_n(\zeta) d\zeta}{(\tau-\zeta)^{\alpha}} \right). \end{aligned}$$

In view of Definition 7 [35], the Haar wavelet fractional derivative’s (HWFD)  $N$ -scale approximation is formulated as follows:

$${}^C D_{\tau}^{\alpha} \phi(\tau) = \frac{1}{\Gamma(1-\alpha)} \sum_{n=0}^N \varphi_n \left( \int_0^{\tau} \frac{\tilde{h}_n(\xi) \tilde{h}_{N-n}(\xi) d\xi}{(\tau-\xi)^{\alpha}} \right).$$

We proceed to make a generalization of the HWFD using the calculus of the  $k$ -symbol [36].

**Definition 1.** The  $k$ -symbol gamma function  $\Gamma_k$ , often known as the motivated gamma function, is formulated as follows:

$$\Gamma_k(\tau) = \lim_{n \rightarrow \infty} \frac{n! k^n (nk)^{\frac{\tau}{k}-1}}{(\tau)_{n,k}}, \quad \Gamma_k(k) = 1,$$

where:

$$(\tau)_{n,k} := \tau(\tau+k)(\tau+2k) \dots (\tau+(n-1)k)$$

and:

$$(\tau)_{n,k} = \frac{\Gamma_k(\tau+nk)}{\Gamma_k(\tau)}.$$

Hence, by using the  $k$ -fractional operator, we have [37]:

$$\begin{aligned} {}^C D_{\tau}^{\alpha} \phi(\tau) &= \frac{1}{\Gamma_k(k-\alpha)} \sum_{n=0}^N \varphi_n \left( \int_0^{\tau} \frac{\tilde{h}_n(\xi) \tilde{h}_{N-n}(\xi) d\xi}{(\tau-\xi)^{\alpha/k}} \right) \\ &\approx \frac{1}{\Gamma_k(k-\alpha)} \sum_{n=0}^N \varphi_n \left( \int_0^{\tau} \frac{\tilde{h}_N(\xi) d\xi}{(\tau-\xi)^{\alpha/k}} \right) \\ &= \frac{\tilde{h}_N(\tau)}{\Gamma_k(k-\alpha)} \sum_{n=0}^N \varphi_n \left( \int_0^{\tau} \frac{d\xi}{(\tau-\xi)^{\alpha/k}} \right) \\ &= \frac{\tilde{h}_N(\tau)}{\Gamma_k(k-\alpha)} \left( \frac{\tau^{1-\alpha/k}}{1-\alpha/k} \right) \sum_{n=0}^N \varphi_n \\ &= \Phi_N^{\top} H_N(k, \alpha; \tau), \end{aligned}$$

where the integral  $\left( \int_0^{\tau} \frac{\tilde{h}_{kn}(\xi) \tilde{h}_{N-kn}(\xi) d\xi}{(\tau-\xi)^{\alpha/k}} \right)$  is the  $k$ -symbol-symmetric operational matrix,  $\Phi_N^{\top} = [\varphi_0, \dots, \varphi_N]$  is the  $ND$ -row vector, and:

$$H_N(k, \alpha; \tau) = \left[ \frac{\tilde{h}_0(\tau)}{\Gamma_k(k-\alpha)} \left( \frac{\tau^{1-\alpha/k}}{1-\alpha/k} \right), \dots, \frac{\tilde{h}_N(\tau)}{\Gamma_k(k-\alpha)} \left( \frac{\tau^{1-\alpha/k}}{1-\alpha/k} \right) \right]^{\top}.$$

By considering the discrete form of the Haar function  $\tilde{h}_0, \dots, \tilde{h}_N$ , we obtain:

$$H_N(k, \alpha) = \left[ \frac{\tilde{h}_0}{\Gamma_k(k-\alpha)} \left( \frac{N^{1-\alpha/k}}{1-\alpha/k} \right), \dots, \frac{\tilde{h}_N}{\Gamma_k(k-\alpha)} \left( \frac{N^{1-\alpha/k}}{1-\alpha/k} \right) \right]^{\top}.$$

For example, the  $2D - k$  symbol Haar matrix is given by:

$$\begin{aligned} H_2(k, \alpha) &= \frac{1}{\Gamma_k(k-\alpha)} \left( \frac{2^{1-\alpha/k}}{1-\alpha/k} \right) \begin{bmatrix} 1 & 1 \\ 1 & -1 \end{bmatrix} \\ &= \begin{bmatrix} \frac{2^{1-\alpha/k}}{\Gamma_k(1+k-\alpha)} & \frac{2^{1-\alpha/k}}{\Gamma_k(1+k-\alpha)} \\ \frac{2^{1-\alpha/k}}{\Gamma_k(1+k-\alpha)} & -\frac{2^{1-\alpha/k}}{\Gamma_k(1+k-\alpha)} \end{bmatrix}, \quad k \geq \alpha. \end{aligned}$$

Obviously, we obtain the original Haar matrix when  $k = \alpha$ .

A numerical example is given as follows when  $\alpha = 0.5, k = 1, 2, 3$ :

$$H_2(1, 1) = H_2(0.5, 0.5) = \begin{bmatrix} 1 & 1 \\ 1 & -1 \end{bmatrix}, H_2(1, 0.5) = \begin{bmatrix} 1.59577 & 1.59577 \\ 1.59577 & -1.59577 \end{bmatrix}$$

$$H_2(2, 0.5) = \begin{bmatrix} 1.2651 & 1.2651 \\ 1.2651 & -1.2651 \end{bmatrix}, H_2(3, 0.5) = \begin{bmatrix} 0.5361 & 0.5361 \\ 0.5361 & -0.5361 \end{bmatrix}.$$

Note that the best result is obtained when the value of  $\alpha$  is close to the value of  $k$ .

#### 4. Proposed DIS

Several computer-aided dental identification systems (DIS) are available to offer specific tasks for identifications. These systems work on the basis that human dental images have different features that make them suitable for dental feature extraction. However, some of these dental identification systems are still manually carried out. Most of these DISs are designed to provide accurate identification results with minimum human intervention. At a high level of abstraction, the functionality of the DIS can be used for the identification of a subject. In this section, the main components of the proposed DIS are the training phase and the testing phases, which are briefly described. Each phase includes three components in the DIS, which are: the digital image database (DID), feature extraction, and ARs mining, as shown in Figure 1 for the training phase and Figure 2 for the testing phase.

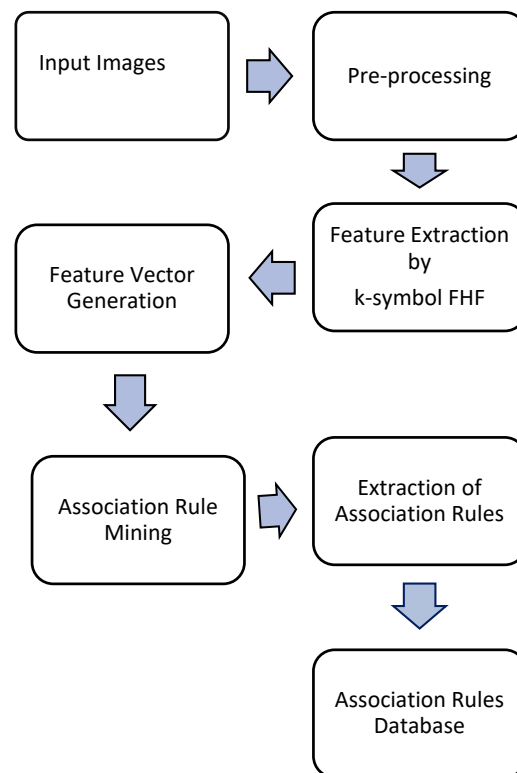


**Figure 1.** The steps for the proposed DIS in the training phase.

The proposed DIS comprises the following three phases: the training phase, testing phase, and query phase. These phases share the same pre-processing and feature extraction algorithms.

The primary concept behind the suggested DIS system is based on the premise that each tooth in a human dental image has a unique property. These features vary from human dental image to human dental image. A DIS system method is developed in this article to extract the distinctive tooth features from the various human dental images and to discover relationship documentations between these images to identify the humanoid teeth

input image. During the preparation stage, the discrete wavelet transform's k-symbol FHF is used to extract the image texture features. Every person's dental features are processed using a sub-band of wavelet coefficient images that have been filtered. The dental texture is represented by the wavelet coefficients. The textural features that are recovered are then used to derive the ARs that, in data mining, represent all human dental images. In the challenging stage of the suggested DIS, all of the extracted images from the training phase are saved in a database and utilized to find the nearest human dental image using the AR algorithm's lowest distance matching. The phases for the suggested DIS are as follows:

1. Step1: Use image cropping and contrast enhancement as part of the pre-processing of the input images to define the area of interest (ROI) for the image extraction step.
2. Step 2: extraction of features from teeth images.
3. Step 3: create image vector.
4. Step 4: employ AR mining utilizing the Apriori algorithm.
5. Step 5: extraction of ARs.

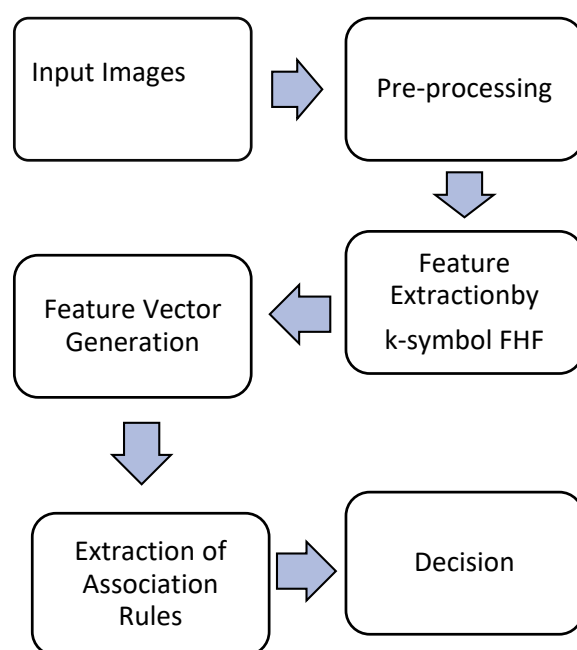


**Figure 2.** The steps for the proposed DIS in the testing phase.

#### 4.1. Data Pre-Processing

Image mining normally deals with huge images in the databases, which requires long times and high costs for data analysis [38]. These databases include a lot of noise, which represents unwanted changes in pixel values caused by various image acquisition factors.

The noise data often produce chaos in the mining process with respect to the quality and efficiency. In the case of mining an image, pre-processing is considered to be a main step in removing noise, and it makes the hidden information more useful and obvious. The key problem is how to quickly process image data that is represented by image features such as texture, color, and shape. For image mining, extracting many features enhances the final mining result. Image features such as the texture, color, and edges are widely used and are considered to be important features in image mining. Different methods such as retrieval and image classification are applied on the extracted feature vectors for image mining to obtain valuable information.

Artifacts that result from the image capturing process may be present in the input images. This procedure is error-prone because the sensor receives many inputs from various independent detectors. The severity of the artifacts may vary from device to device, but generally artifacts degrade the quality of the captured image and may affect the

feature extraction process. Thus, image pre-processing is often needed to reduce the effects of artifacts.

In this study, all dental images were pre-processed to reduce the data size, which sped up the processing by improving the accuracy of the feature extraction. Histogram equalization (HE) was used to improve the contrast in the dental images in this stage. The goal of the HE method, a nonlinear procedure, is to enhance image brightness such that it is appropriate for the humanoid optical scheme. The HE procedure aims to adjust the value of an image in such a mode as to yield an image with a compliment histogram, where all levels have equal probability. The HE is calculated by including the comparable pixel greatness values and dividing these values by the total number of obtainable pixels. Mostly, HE is a list of all pixel values in an image.

The histogram equalization process steps are as follows:

- 1- Convert the input dental image into a grayscale image.
- 2- Calculate the frequency of the pixel value occurrence for the input dental image.
- 3- Find the cumulative occurrence of the pixel value occurrence.

Multiply by the extreme pixel value of the supplied teeth image after dividing the increasing occurrences from step 3 by the overall sum of pixels.

The second pre-processing algorithm is image cropping, which is used to lower the image noise and enhance the feature extraction process of preserving the important regions of the input teeth image.

#### 4.2. Feature Extraction

The feature extraction model involves extracting the useful set of features from the pre-processed images. To differentiate between human dental images, the extracted features are used. The major feature extraction method employed by the suggested system was based on k-symbol FHF wavelet transformations. The input dental image is cropped before the wavelet feature extraction step in order to decrease the magnitude of the teeth image and to identify the domain of attentiveness. In this step, these input images are subjected to a 2D wavelet transformation utilizing k-symbol FHF wavelet decomposition, which processes data by computing the averages and differences of adjacent elements. Prior to operating on adjacent vertical elements, the k-symbol FHF wavelet operates on adjacent horizontal elements. It computes the k-symbol FHF wavelet transform for N items.

The discrete wavelet transform (DWT) on the k-symbol FHF wavelet at level 2 is used in step 2 of the proposed DIS to extract the features from dental images and produce the approximation coefficients matrix cA. The extracted features from all the gathered dental images are used to create the final feature vector. The pre-dealing out step contains an adaptation of a color teeth image into to grayscale image by applying the weighted technique [39]:

$$I(i, j) = 0.99R + 0.587G + 0.114B \quad (1)$$

where  $I(i, j)$  is the grayscale image and  $R$ ,  $G$ , and  $B$  are the triple-color domain images.

The proposed feature extraction process is described as follows:

1. Read the dental image and convert it to a grayscale image.
2. Using the 2D wavelet decomposition-type k-symbol FHF wavelet and then calculating the "approximation coefficients" matrix cA with the horizontal (cH), vertical (cV), and diagonal (cD) "detail coefficient" matrixes. These are obtained from the wavelet decomposition of the input image.
3. Store the cA matrix as an array in a feature vector. In the experiments, 12 features are extracted for every contribution image, which are signified by the estimate coefficients matrix cA at level 2 of the k-symbol FHF wavelet.
4. Save the extracted images in a preparation database.
5. Repeat the stages from 1 to 3 for all input dental images.
6. End.

When all the extracted dental image features are obtained, the features are saved in the training features database. The database contains 12 features that reflect the 12 features that were taken from the k-symbol FHF wavelet-based approximation coefficients matrix, which is cA of each dental image at level 2. The final features can be used for AR mining once all the features have been retrieved.

#### 4.3. Association Rule Mining

Recently, AR mining has become a hot research topic in the data mining field. The core of the suggested DIS algorithm is made up of the ARs that were retrieved from the dental images. The purpose of AR mining is to display the commonly occurring features in each dataset to identify the most intriguing relationships among a large collection of images. Finding frequent item sets that produce powerful ARs that fall below the minimal confidence level is the goal of AR mining. The Apriori algorithm may be used to complete the AR extraction procedure. The Apriori method, which relies on calculating the frequency number for each item transaction in the database regardless of the quantity of the items, is successful for frequent item sets. Several advancements have been made to the standard AR mining algorithm, Apriori. In step 4 of the proposed DIS, the final feature vector of the input dental image is submitted to AR generation. This section introduces search constraints to find only predictive association rules and to reduce the number of patterns. The problem of discovering ARs is decomposed into two basic sub-problems [40]:

The following algorithm describes the steps of the AR algorithm [41]:

- 1- Finding all frequent item sets, X, such that  $\text{support}(X) \geq$  the support threshold.

The AR is a relation of the type  $(A) \rightarrow (B)$  in this phase, where (A) and (B) are piece arrays. The (A) item is referred to as the statute's figure, while the (B) item is referred to as the rule's head. The rules that the mining process returns are determined by the support and confidence rates. The "Support" value describes how frequently an AR is relevant to given transaction data, while the "Confidence" describes how often items in B are found in transactions that have (A).

Instructions are of the formula  $(A) \rightarrow (B)$ , for example: [image values]  $\rightarrow$  [another image value], where "support" = minSup (minimum support threshold) and "Confidence" = minConf (minimum confidence threshold). The "Support" is the fraction of transactions that contain both (A) and (B):  $\text{support}(A, B) = P(A, B)$ . The "Confidence" is the portion of transactions where items in B are found in transactions that contain (A):  $\text{confidence}(A, B) = P(B | A)$ .

The steps of the Apriori algorithm are as follows:

1. Determine the dental image database item set's level of support and then determine the minimal level of support and confidence.
2. Pick every higher support value available in the image database.
3. Find every rule with a higher confidence value.
4. Arrange the rules in descending priority.

The pseudo code of the Apriori algorithm is illustrated in Figure 3 [41]:

The aim of mining ARs is to discover all rules that have "Support and Confidence" values greater than the minimum Support and minimum Confidence threshold values, which are specified by the user.

The transaction features of all input dental images are given as an input to the Apriori algorithm to generate the required ARs.

The standard methodology for evaluating the accuracy of similarity rule values is given by:

- 1- If the image satisfies all of the rules, then the values of the image feature match the values of the instructions in the training set.
- 2- The types of stages that will be developed depend on how well the image feature values meet the guidelines.
- 3- If the image features do not fulfill any part of the instructions, the values of the image feature do not match the procedures [42].

Sorting the image into the class with the most applicable rules comes first when developing a classification system. If the number of rules retrieved from each class is balanced, this classification would function effectively; otherwise, more fine-tuning of the classification system is required.

L<sub>k</sub>: frequent k-itemset, satisfy minimum support

C<sub>k</sub>: candidate k-itemset, possible frequent k-itemsets

```

L1 = {frequent 1-itemsets};
for (k=2; Lk-1 ≠ 0; k++) do begin
  Ck = apriori-gen (Lk-1);
  for each transactions t ∈ D do begin//scan DB
    Ct = subset (Ck, t) //get the subsets of t that are candidates
    for each candidate c ∈ Ct do
      c.count++; //increment the count
    end
  Lk = {c ∈ Ck | c.count ≥ minsup}
end

return Uk Lk;

```

**Figure 3.** The pseudo code of the Apriori algorithm.

#### 4.4. Testing Phase

The following actions are taken in this phase:

1. Type in the mock dental image.
2. The system uses the same training phase technique to extract the test image's features before obtaining the ARs for image recognition.

#### 4.5. Inquiry Stages

When a user provides an image of a dental subject, the process of recognizing that image begins. Following dental identification, a "short" selection of candidate images is supplied to the dental expert, together with reference data that have been acquired from the dental image repository. This phase is used for the following phases in querying:

- a. Dental image acquisition;
- b. Dental image pre-processing;
- c. Dental image feature extraction;
- d. Association rules extraction.

### 5. Experimental Results

This study was implemented using Matlab 2020b with Windows 10 using a 64-bit computer with an Intel(R) Core (TM) i7-4810MQ CPU with 8 GB of RAM.

The suggested AR-based image mining approach was tested using the collected dental image database. The dental images used to carry out the proposed study were extracted from the digitized dental image database provided by the local dental center. The images were chosen with different qualities to test the performance of the proposed Apriori-based dental identification system. In Figure 4, a sample of the gathered image collection is displayed.



**Figure 4.** Sample of images collected in the database.

### 5.1. Assessment Standards

The evaluating performance of the proposed DIS was measured by the identification accuracy. The identification accuracy is formulated as the percentage ratio between the number of accurately identified dental images and the total number of dental images, which is defined by the following formula:

$$\text{Identification accuracy} = \frac{\text{The number of corrected identified images}}{\text{Total number of images}} \quad (2)$$

### 5.2. The Results

#### 5.2.1. Result of Pre-Processing

Several tests were carried out to evaluate the proposed dental identification system accuracy. The image pre-processing step was required to increase the image quality and make the feature extraction phase more efficient. When the data to be mined are noisy, pre-processing is always required. Before the feature extraction step, the pre-processing procedures were used for all images. The results of the pre-processing stage are illustrated in Figure 5, which includes the image enhancement using the histogram equalization approach (HE) (Figure 5B) and image cropping (Figure 5C).

The HE method's pre-processing procedures for enhancing image contrast produced greater enhancement outcomes in terms of image quality than the original input images. The HE model's overall contrast enhancement made the architecture of the medical images more distinct. This pre-processing created the increased image capabilities to effectively display minute dental features.

The white portion surrounding the teeth was cut in the second stage of pre-processing. Cropping was performed after image enhancement to highlight the region of interest within the image. Cropping was performed automatically by sweeping across the image and cutting horizontally and vertically, as illustrated in Figure 5C. The image pre-processing phase for image cropping decreased the dental image's processing area, which in turn minimized any image noise present in the input image. The final stage of pre-processing comprised the weighted conversion of a color dental image to a grayscale image (Figure 5D).

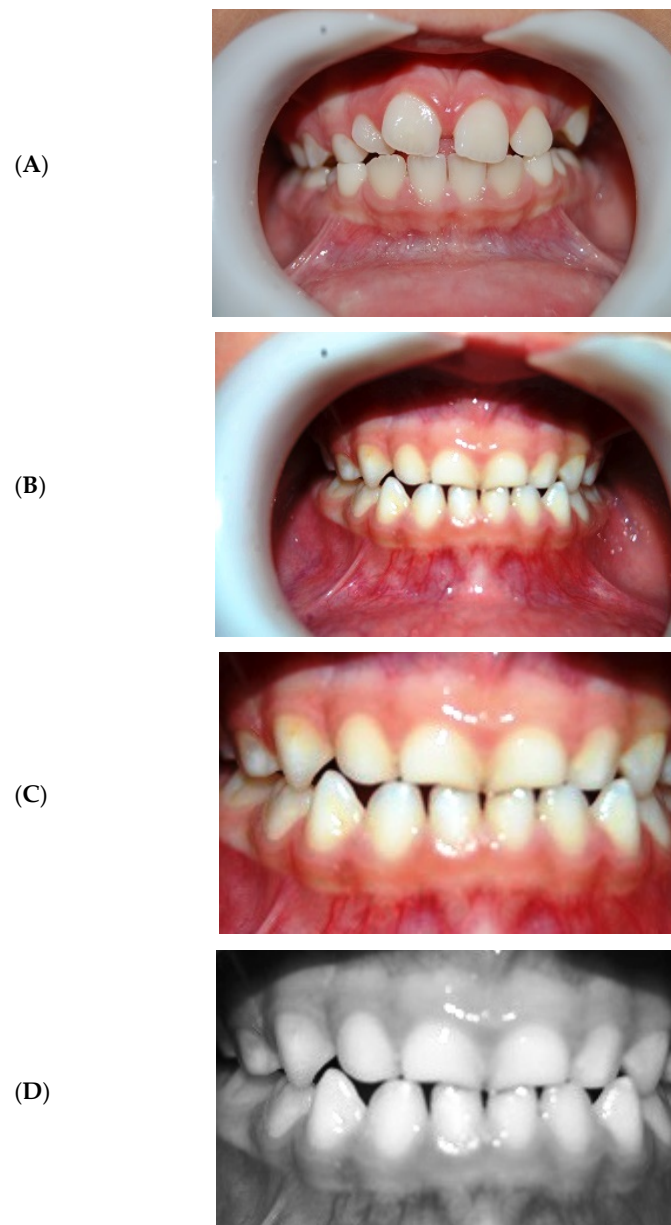
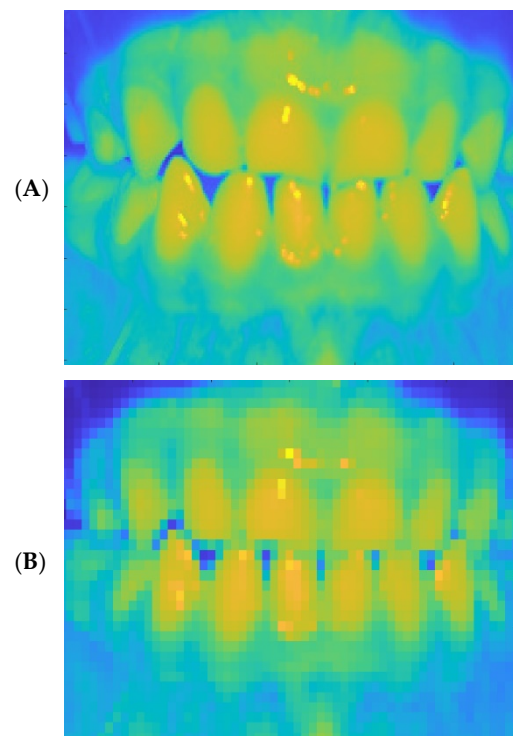


**Figure 5.** Cropping. (A) Input image, (B) contrast enhancement, (C) cropped enhanced image, (D) grayscale cropped enhanced image.

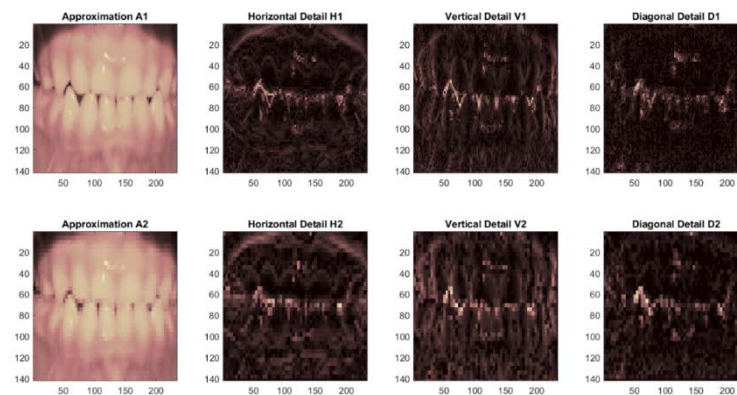
### 5.2.2. Result of Image Extraction Phase

The wavelet image decomposition provided a simple description of the input image. Each sub-image contained information of a certain scale and orientation that was divided properly. To extract image features, the original image was divided into approximation and detail coefficients. The features were extracted from the cropped images in step 2 of the proposed DIS by obtaining the approximation coefficients of the  $k$ -symbol FHF wavelet decomposition. After the dental image features were extracted, they were saved in the training features database. After all the features were extracted, the final features were used for association rule mining.

For each dental input image, the extracted features were created as feature vectors of 12 features. Figures 6 and 7 show the resulting images of the 2D  $k$ -symbol FHF wavelet with the extracted first- and second-level approximation coefficients and detail coefficients, respectively.



**Figure 6.** Obtaining the 2D k-symbol FHF transform to level 2. (A) Input image, (B) view of the k-symbol FHF approximation.



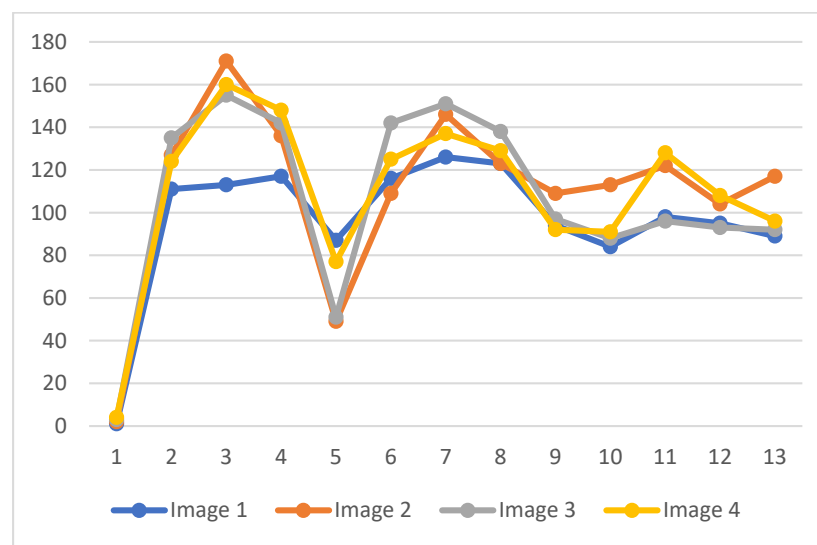
**Figure 7.** The extraction of the first and second levels of the approximation coefficients and detail coefficients.

Table 1 is an illustration of a final feature extraction sample. The columns reflect the 12 features that were retrieved from the approximation coefficients matrix,  $cA$ , of each dental image at level 2 using the k-symbol FHF wavelet, while the rows represent the features of the dental images. Subsequently, all the images were retrieved; the final images can be utilized for suggestion rule mining.

Figure 8 shows the robust texture features that were recovered from certain sample dental image wavelet approximation coefficients. This example demonstrates the close relationship between the image features that are utilized to derive the ARs. Following the feature extraction process, the extracted texture features were saved in the training database together with the ARs that were extracted from each image.

**Table 1.** Example of the concluding image vector.

Images	F1	F2	F3	F4	F5	F6	F7	F8	F9	F10	F11	F12
1	111	113	117	87	116	126	123	94	84	98	95	89
2	127	171	136	49	109	146	123	109	113	122	104	117
3	135	155	142	51	142	151	138	97	88	96	93	92
4	124	160	148	77	125	137	129	92	91	128	108	96
5	114	150	113	83	114	147	126	104	120	132	106	119
6	120	129	96	92	140	123	118	76	119	119	109	110
7	94	140	116	58	121	145	151	105	117	136	133	94
8	117	170	163	85	109	114	117	107	101	112	110	98
9	135	170	163	95	138	152	146	97	106	82	95	77
10	99	149	141	81	111	141	140	104	96	124	107	102

**Figure 8.** Comparison of the k-symbol FHF wavelet approximation coefficients of the sample images.

### 5.2.3. Result of Association Rules Step

The step 3, the AR mining procedure was achieved by utilizing the Apriori algorithm. A sample of ARs generated by the proposed algorithm are illustrated in Table 2. The rows indicate dental image features, while the columns reflect the 12 features extracted from the approximation coefficients matrix, cA, of each dental image at level 2. The description of the first row is as follows: according to these criteria, images with the attributes 77, 91, 92, 124, 125, 129, 137, and 148 are more likely to be dental images due to the achieved thresholds of support = 25% and confidence = 100%.

**Table 2.** Samples of mined ARs.

77, 91, 92, 124, 125, 129, 137, 148, → 160, support: $2.500000 \times 10^{-1}$ , confidence: 1
77, 91, 92, 124, 125, 129, 137, 160, → 148, support: $2.500000 \times 10^{-1}$ , confidence: 1
77, 91, 92, 124, 125, 129, 148, 160, → 137, support: $2.500000 \times 10^{-1}$ , confidence: 1
77, 91, 92, 124, 125, 137, 148, 160, → 129, support: $2.500000 \times 10^{-1}$ , confidence: 1
77, 91, 92, 124, 129, 137, 148, 160, → 125, support: $2.500000 \times 10^{-1}$ , confidence: 1
77, 91, 92, 125, 129, 137, 148, 160, → 124, support: $2.500000 \times 10^{-1}$ , confidence: 1
77, 91, 124, 125, 129, 137, 148, 160, → 92, support: $2.500000 \times 10^{-1}$ , confidence: 1
77, 92, 124, 125, 129, 137, 148, 160, → 91, support: $2.500000 \times 10^{-1}$ , confidence: 1

**Table 2.** *Cont.*

91, 92, 124, 125, 129, 137, 148, 160, → 77, support: $2.500000 \times 10^{-1}$ , confidence: 1
84, 87, 94, 111, 113, 116, 117, 123, → 126, support: $2.500000 \times 10^{-1}$ , confidence: 1
84, 87, 94, 111, 113, 116, 117, 126, → 123, support: $2.500000 \times 10^{-1}$ , confidence: 1
84, 87, 94, 111, 113, 116, 123, 126, → 117, support: $2.500000 \times 10^{-1}$ , confidence: 1
84, 87, 94, 111, 113, 117, 123, 126, → 116, support: $2.500000 \times 10^{-1}$ , confidence: 1
84, 87, 94, 111, 116, 117, 123, 126, → 113, support: $2.500000 \times 10^{-1}$ , confidence: 1
84, 87, 94, 113, 116, 117, 123, 126, → 111, support: $2.500000 \times 10^{-1}$ , confidence: 1
84, 87, 111, 113, 116, 117, 123, 126, → 94, support: $2.500000 \times 10^{-1}$ , confidence: 1
84, 94, 111, 113, 116, 117, 123, 126, → 87, support: $2.500000 \times 10^{-1}$ , confidence: 1
87, 94, 111, 113, 116, 117, 123, 126, → 84, support: $2.500000 \times 10^{-1}$ , confidence: 1

The results prove that dental image mining is achievable and that the Apriori method produced an adequate number of rules. As a result, the suggested DIS increased confidence in the dental image identification process. However, the proposed technique does not employ any parameter optimization, which we will address in future work.

#### 5.2.4. Result of Testing Phase

The testing phase was used to validate the dental identification accuracy of the DIS. The result of the training stage contained rules learned from the input feature patterns. For the proposed DIS, the model was trained to test any input dental image. The output of the testing phase was in terms of a predictive measure, which was in the form of evaluation metrics of dental image identification accuracy. The testing image was used to check the identification accuracy after the DIS had been trained. The testing phase process involved image pre-processing, image feature extraction by the k-symbol FHF wavelet, and the AR extraction. The ratio of similarity between the ARs for testing dental images and the ARs contained in the dental image association rules database was measured by the testing dental image identification accuracy. Table 3 shows the outcomes of dental image identification for one sample of a dental image, including the number of rules present in the sub-class, the number of rules entered from the teeth image, and the degree of similarity between the AR for the test teeth image and the ARs kept in the database of dental imaging.

**Table 3.** Results of dental identification for one sample of dental images.

Images	No. of Rules Input in Image	No. of Rules Input in Image	Count Rule %	Similarity Matching %
First	23	6	5	5/6 = 83.33
Second	44	8	7	6/8 = 75.0
Third	26	6	5	7/8 = 87.5
Fourth	32	7	6	6/7 = 85.71
Fifth	48	8	7	7/8 = 87.5
Average				83.808%

The proposed DIS based on k-symbol FHF wavelet transforms achieved an average identification accuracy of 80%. The proposed DIS algorithm in this study mainly improved the dental identification system based on the Apriori algorithm, which was envisioned to resolve the boundaries of dental rule mining. The proposed extracted features of dental images produced satisfactory results in this study. The most useful features were extracted utilizing two-level k-symbol FHF wavelet transformations.

The current study included the following limitations:

- 1- The images utilized to assess the applicability of this study came from a single source and were obtained by several technologies.
- 2- The small dataset that was employed had an impact on the proposed identification model's accuracy. The vast dataset, on the other hand, will help to construct a more robust dental identification model.

As a result, we conclude that the proposed Apriori-based dental identification model is effective at recognizing dental images and will be useful in supporting clinicians in identification. This model produced good findings in terms of time and accuracy, and it is a reliable and effective tool as a dental identification system. The mentioned methodology was used to create an identification dental system based on association rule classification with the new proposed feature extraction of two-level k-symbol FHF wavelet transforms.

## 6. Conclusions

The key factor that affects classification accuracy is the choice of related features from the input images. The proposed k-symbol FHF wavelet transform feature extraction model helped enhance the performance of the Apriori-based dental identification. This study explored the use of an AR algorithm to build a dental identification system. Dental image features are extracted, and frequent feature patterns are found in images using AR mining with an Apriori algorithm. The proposed method learns the rules in the dental database. The rule mining process made the proposed DIS simple and efficient. The performance of the proposed DIS was evaluated using the MATLAB platform. Experimentation using a collected dental database was implemented to display the efficient performance of the proposed DIS method. For future work, more experimentation using a different database with different image feature extraction will be performed to obtain more enhancement in the identification results. Moreover, the ARs will be optimized utilizing one of the optimization processes to enhance the accuracy of the dental identification system.

**Author Contributions:** Conceptualization, M.H.A. and R.W.I.; methodology, N.M.G.A.-S. and R.W.I.; software, N.M.G.A.-S.; validation, M.H.A. and R.W.I.; formal analysis, N.M.G.A.-S. and R.W.I.; investigation, N.M.G.A.-S.; resources, M.H.A.; data creation, N.M.G.A.-S.; writing—original draft preparation, R.W.I.; funding acquisition, M.H.A. All authors have read and agreed to the published version of the manuscript.

**Funding:** This research received no external funding.

**Data Availability Statement:** The anterior open bite images for this study were obtained from the local dental center. <https://github.com/fjawadif/Open-bite-images> (accessed on 1 November 2022).

**Conflicts of Interest:** The authors declare no conflict of interest.

## References

1. Teng, X.; Gong, Y. Research on application of machine learning in data mining. *IOP Conf. Ser. Mater. Sci. Eng.* **2018**, *392*, 062202. [[CrossRef](#)]
2. Taleb, I.; Dssouli, R.; Serhani, M.A. Big Data Pre-Processing: A Quality Framework. In Proceedings of the 2015 IEEE International Congress on Big Data, New York, NY, USA, 27 June–2 July 2015; pp. 191–198.
3. Yin, P.-Y.; Li, S.-H. Content-Based image retrieval using association rule mining with soft relevance feedback. *J. Vis. Commun. Image Represent.* **2006**, *17*, 1108–1125. [[CrossRef](#)]
4. Veroneze, R.; Cruz Tfaile Corbi, S.; Roque da Silva, B.; Rocha, C.d.; Maurer-Morelli, C.V.; Perez Orrico, S.R.; Cirelli, J.A.; Von Zuben, F.J.; Mantuanelli Scarel-Caminaga, R. Using association rule mining to jointly detect clinical features and differentially expressed genes related to chronic inflammatory diseases. *PLoS ONE* **2020**, *15*, e0240269. [[CrossRef](#)] [[PubMed](#)]
5. Deshmukh, J.; Bhosle, U. Image mining using association rule for medical image dataset. *Procedia Comput. Sci.* **2016**, *85*, 117–124. [[CrossRef](#)]
6. Zeng, N.; Xiao, H. Inferring implications in semantic maps via the Apriori algorithm. *Lingua* **2020**, *239*, 102808. [[CrossRef](#)]
7. Nahar, J.; Imam, T.; Tickle, K.S.; Chen, Y.-P.P. Association rule mining to detect factors which contribute to heart disease in males and females. *Expert Syst. Appl.* **2013**, *40*, 1086–1093. [[CrossRef](#)]
8. Chaves, R.; Ramirez, J.; Górriz, J.; Puntonet, C.G.; Alzheimer's Disease Neuroimaging Initiative. Association rule-based feature selection method for Alzheimer's disease diagnosis. *Expert Syst. Appl.* **2012**, *39*, 11766–11774. [[CrossRef](#)]

9. Lee, A.J.; Liu, Y.-H.; Tsai, H.-M.; Lin, H.-H.; Wu, H.-W. Mining frequent patterns in image databases with 9D-SPA representation. *J. Syst. Softw.* **2009**, *82*, 603–618. [[CrossRef](#)]
10. Lee, A.J.; Hong, R.-W.; Ko, W.-M.; Tsao, W.-K.; Lin, H.-H. Mining spatial association rules in image databases. *Inf. Sci.* **2007**, *177*, 1593–1608. [[CrossRef](#)]
11. Fahmy, G.; Nassar, D.; Haj-Said, E.; Chen, H.; Nomir, O.; Zhou, J.; Howell, R.; Ammar, H.H.; Abdel-Mottaleb, M.; Jain, A.K. Towards An Automated Dental Identification System (ADIS). In Proceedings of the International Conference on Biometric Authentication, Hong Kong, China, 15–17 July 2004; pp. 789–796.
12. Ibrahim, R.W.; Yahya, H.; Mohammed, A.J.; Al-Saidi, N.M.; Baleanu, D. Mathematical Design Enhancing Medical Images Formulated by a Fractal Flame Operator. *Intell. Autom. Soft Comput.* **2022**, *32*, 937–950. [[CrossRef](#)]
13. Jiao, Q.; Liu, M.; Ning, B.; Zhao, F.; Dong, L.; Kong, L.; Hui, M.; Zhao, Y. Image Dehazing Based on Local and Non-Local Features. *Fractal Fract.* **2022**, *6*, 262. [[CrossRef](#)]
14. Zhang, Y.; Liu, T.; Yang, F.; Yang, Q. A Study of Adaptive Fractional-Order Total Variational Medical Image Denoising. *Fractal Fract.* **2022**, *6*, 508. [[CrossRef](#)]
15. Zhang, X.; Dai, L. Image Enhancement Based on Rough Set and Fractional Order Differentiator. *Fractal Fract.* **2022**, *6*, 214. [[CrossRef](#)]
16. Zhang, Y.; Yang, L.; Li, Y. A Novel Adaptive Fractional Differential Active Contour Image Segmentation Method. *Fractal Fract.* **2022**, *6*, 579. [[CrossRef](#)]
17. Al-Saidi, N.M.; Al-Bundi, S.S.; Al-Jawari, N.J. A hybrid of fractal image coding and fractal dimension for an efficient retrieval method. *Comput. Appl. Math.* **2018**, *37*, 996–1011. [[CrossRef](#)]
18. Sahu, M.; Shrivastava, M.; Rizvi, M. Image Mining: A New Approach for Data Mining Based on Texture. In Proceedings of the 2012 Third International Conference on Computer and Communication Technology, Allahabad, India, 23–25 November 2012; pp. 7–9.
19. Rajendran, P.; Madheswaran, M. An improved image mining technique for brain tumour classification using efficient classifier. *arXiv* **2010**, arXiv:1001.1988.
20. Khodaskar, A.; Ladhake, S. Image Mining: An Overview of Current Research. In Proceedings of the 2014 Fourth International Conference on Communication Systems and Network Technologies, Bhopal, India, 7–9 April 2014; pp. 433–438.
21. Gajjar, T.; Chauhan, N. A review on image mining frameworks and techniques. *Int. J. Comput. Sci. Inf. Technol.* **2012**, *3*, 4064–4066.
22. Dey, N.; KarĀca, W.B.A.; Chakraborty, S.; Banerjee, S.; Salem, M.A.; Azar, A.T. Image mining framework and techniques: A review. *Int. J. Image Min.* **2015**, *1*, 45–64. [[CrossRef](#)]
23. Zhang, J.; Hsu, W.; Lee, M.L. Image Mining: Issues, Frameworks and Techniques. In Proceedings of the 2nd ACM SIGKDD International Workshop on Multimedia Data Mining (MDM/KDD'01), San Francisco, CA, USA, 26 August 2001.
24. Agarwal, S.; Singh, O.; Nagaria, D. Analysis and comparison of wavelet transforms for denoising MRI image. *Biomed. Pharmacol. J.* **2017**, *10*, 831–836. [[CrossRef](#)]
25. Hsu, W.; Lee, M.L.; Zhang, J. Image mining: Trends and developments. *J. Intell. Inf. Syst.* **2002**, *19*, 7–23. [[CrossRef](#)]
26. Yun, J.; Zhanhuai, L.; Yong, W.; Longbo, Z. Joining Associative Classifier for Medical Images. In Proceedings of the Fifth International Conference on Hybrid Intelligent Systems (HIS'05), Rio de Janeiro, Brazil, 6–9 November 2005; p. 6.
27. Tseng, V.S.; Wang, M.-H.; Su, J.-H. A New Method for Image Classification by Using Multilevel Association Rules. In Proceedings of the 21st International Conference on Data Engineering Workshops (ICDEW'05), Tokyo, Japan, 3–4 April 2005; p. 1180.
28. Ribeiro, M.X.; Traina, A.J.; Traina, C.; Azevedo-Marques, P.M. An association rule-based method to support medical image diagnosis with efficiency. *IEEE Trans. Multimed.* **2008**, *10*, 277–285. [[CrossRef](#)]
29. Ribeiro, M.X.; Bugatti, P.H.; Traina, C., Jr.; Marques, P.M.; Rosa, N.A.; Traina, A.J. Supporting content-based image retrieval and computer-aided diagnosis systems with association rule-based techniques. *Data Knowl. Eng.* **2009**, *68*, 1370–1382. [[CrossRef](#)]
30. Rajendran, P.; Madheswaran, M. Hybrid medical image classification using association rule mining with decision tree algorithm. *arXiv* **2010**, arXiv:1001.3503.
31. Da Silva, S.F.; Ribeiro, M.X.; Neto, J.d.E.B.; Traina, C., Jr.; Traina, A.J. Improving the ranking quality of medical image retrieval using a genetic feature selection method. *Decis. Support Syst.* **2011**, *51*, 810–820. [[CrossRef](#)]
32. Abdi, M.J.; Giveki, D. Automatic detection of erythematous-squamous diseases using PSO-SVM based on association rules. *Eng. Appl. Artif. Intell.* **2013**, *26*, 603–608. [[CrossRef](#)]
33. Mangat, V.; Vig, R. Dynamic PSO-based associative classifier for medical datasets. *IETE Tech. Rev.* **2014**, *31*, 258–265. [[CrossRef](#)]
34. Aziz, I.; Amin, R. Numerical solution of a class of delay differential and delay partial differential equations via Haar wavelet. *Appl. Math. Model.* **2016**, *40*, 10286–10299. [[CrossRef](#)]
35. Cattani, C. Haar wavelet fractional derivative. *Proc. Est. Acad. Sci.* **2022**, *71*, 55–64. [[CrossRef](#)]
36. Diaz, R.; Pariguan, E. On hypergeometric functions and Pochhammer  $k$ -symbol. *arXiv* **2004**, arXiv:math/0405596.
37. Mubeen, S.; Habibullah, G.  $k$ -Fractional integrals and application. *Int. J. Contemp. Math. Sci.* **2012**, *7*, 89–94.
38. Girija, O.; Elayidom, M.S. Overview of Image Retrieval Techniques. *Int. J. Adv. Res. Comput. Commun. Eng.* **2015**, *4*. [[CrossRef](#)]
39. Woods, R.E.; Eddins, S.L.; Gonzalez, R.C. *Digital Image Processing Using MATLAB*; Pearson: Noida, India, 2009.
40. Ordonez, C. Association rule discovery with the train and test approach for heart disease prediction. *IEEE Trans. Inf. Technol. Biomed.* **2006**, *10*, 334–343. [[CrossRef](#)] [[PubMed](#)]

- 
41. Vyas, R.; KUMAR, L.; Tiwary, U. Exploring spatial ARM (Spatial Association Rule Mining) for geo-decision support system. *J. Comput. Sci.* **2007**, *3*, 1–3. [[CrossRef](#)]
  42. Padmapriya, A.; Maragatham, K. Priority Based Apriori Algorithm for Cancer Prediction Using Fuzzy Classification. *Int. J. Eng. Res. Technol.* **2013**, 2259–2266. [[CrossRef](#)]